Supplemental Fig. 1. Levels of total WBC, RBC, and platelets were counted using a Coulter counter on day 4 post infection in wild type and TLR9-/- mice (A-C). Interferon levels were measured using ELISA (D and E) Lung sections were stained with hematoxylin and eosin on day 7. Sup Fig. 1F shows representative pictures on day 7.

Supplemental Fig. 2. Flow strategy to detect immune cell populations in the BAL.

Supplemental Fig. 3. Western blot analysis of influenza NS1 protein on day 10 post-infection (A and B) and day 14 post infection (C).

Supplemental Fig. 4. UMAP of epithelial cells in the lung (A) and markers to identify specific cell types (B). The identity of infected cells and associated genotype (C) and quantification (D). IPA pathway analysis showing enriched pathway in wild type and TLR9-/- ciliated epithelium (E and F).

Supplemental Fig. 5. UMAP showing an expansion of iMON_Highinfection in infected mice, especially in TLR9-/- lungs.

Supplemental Fig. 6. Violin plots showing the expression levels of specific gene (A). Cell-cell communication analyses were performed using the R package Connectome. Average expression levels of ligands and receptors per cell type were computed across experimental groups. Connectomes were constructed for each experimental group, containing unfiltered lists of edges linking ligand-expressing cells to receptor-expressing cells. Diff-connectome was generated to demonstrate the upregulated receptor-ligand interactions in TLR9 KO cells (B). Human PBMC cell lines were infected with influenza (MOI of 1) and cytokine expressions were measured over the time course using qPCR (C). *, $P < 0.05$, **, $P<0.01$, and ***, $P < 0.005$ using two-way ANOVA.

Supplemental Fig. 7. STAT1 and NFkB pathway signature in immune (A and B) and epithelial cells (C and D) along with respective quantifications on the right.

Supplemental Fig. 8. Apoptosis (A), necroptosis (B), and pyroptosis (C) pathway signatures in immune cells along with respective quantifications on the right.

Supplemental Fig. 9. TLR9 stimulation post viral clearance impairs recovery: Histological analysis of lung tissue sections that were stained with trichrome staining to assess fibrosis (blue color) (A). Wild type mice were infected with influenza virus and randomized into two groups to either receive TLR9 agonist ODN2006 or PBS on day 8 by intranasal route. Body weights were measured every day. # indicates mortality in the ODN2006 on the indicated day (B). Wild type and TLR9-/- mice were infected with 4x dose (40 PFUs) of influenza virus and treated with oseltamivir every day (30 mg/kg) starting on day 1 post infection and until day 9 post infection. Body weights were measured (C). N=4-5 each group in A and 9-10 each group in B. ***, $P<0.005$ using two-way ANOVA with Šídák's multiple comparisons test, n= non-significant, # indicates one death on that day.

Supplemental Fig. 10. Myeloid specific TLR9 deficiency ameliorates lung inflammation without affecting viral clearance. LysM TLR9+/+ and LysM TLR9-/- were infected with influenza virus and euthanized on day 7 or day 14 to measure viral load and inflammation. Viral load was measured by qPCR on day 7 (A). Total WBCs were measured in the BAL samples harvested on day 14 (B) and specific cells were identified in a subset of experiments using flow cytometry (C). **, $P < 0.01$ using Mann-Whitney test and ***, $P < 0.005$ using two-way ANOVA.

Supplemental Fig. 11. TLR9 activity was measured in mouse serum samples that were infected for 4, 7, or 14-days using mouse TLR9 reporter cell line. The data were measured using repeated measures for 6 hours. PBS alone served as a negative control. Day 7 values are statistically significant.

Supplemental Table 1: Raw data that were used to generate all the figures used for this manuscript.

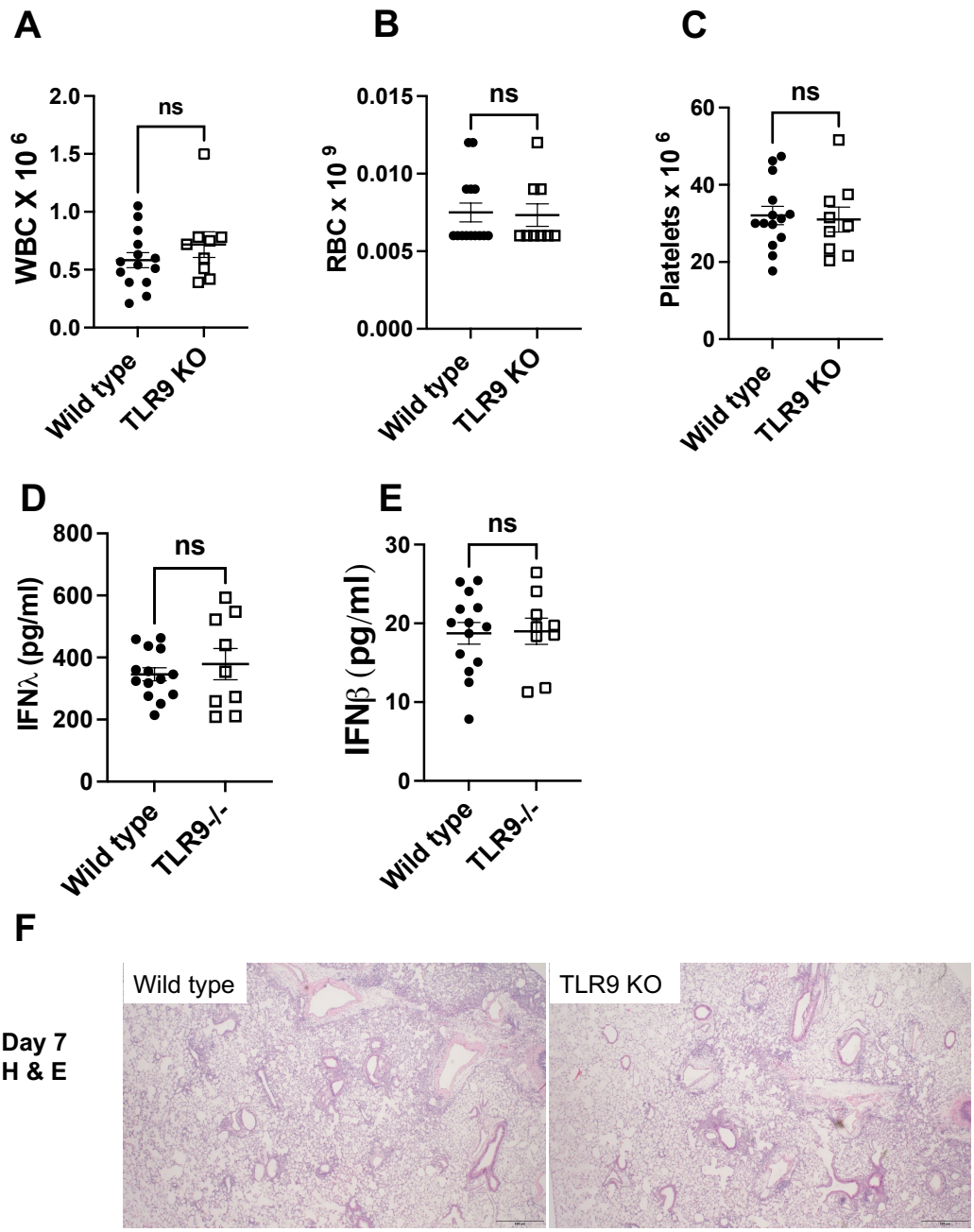

Supplemental Fig. 1. Levels of total WBC, RBC, and platelets were counted using a Coulter counter on day 4 post infection in wild type and TLR9-/- mice (A-C). Interferon levels were measured using ELISA (D and E) Lung sections were stained with hematoxylin and eosin on day 7. Sup Fig. 1F shows representative pictures on day 7.

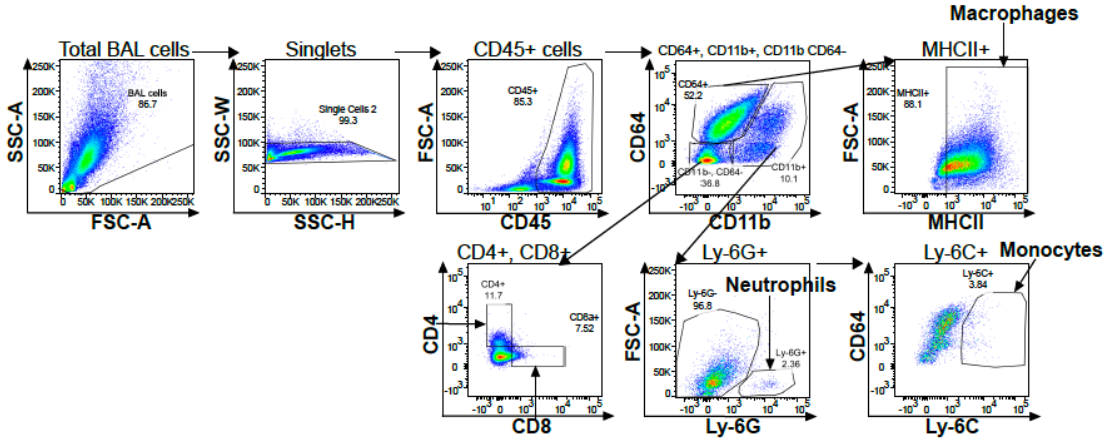

Supplemental Fig. 2. Flow strategy to detect immune cell populations in the BAL.

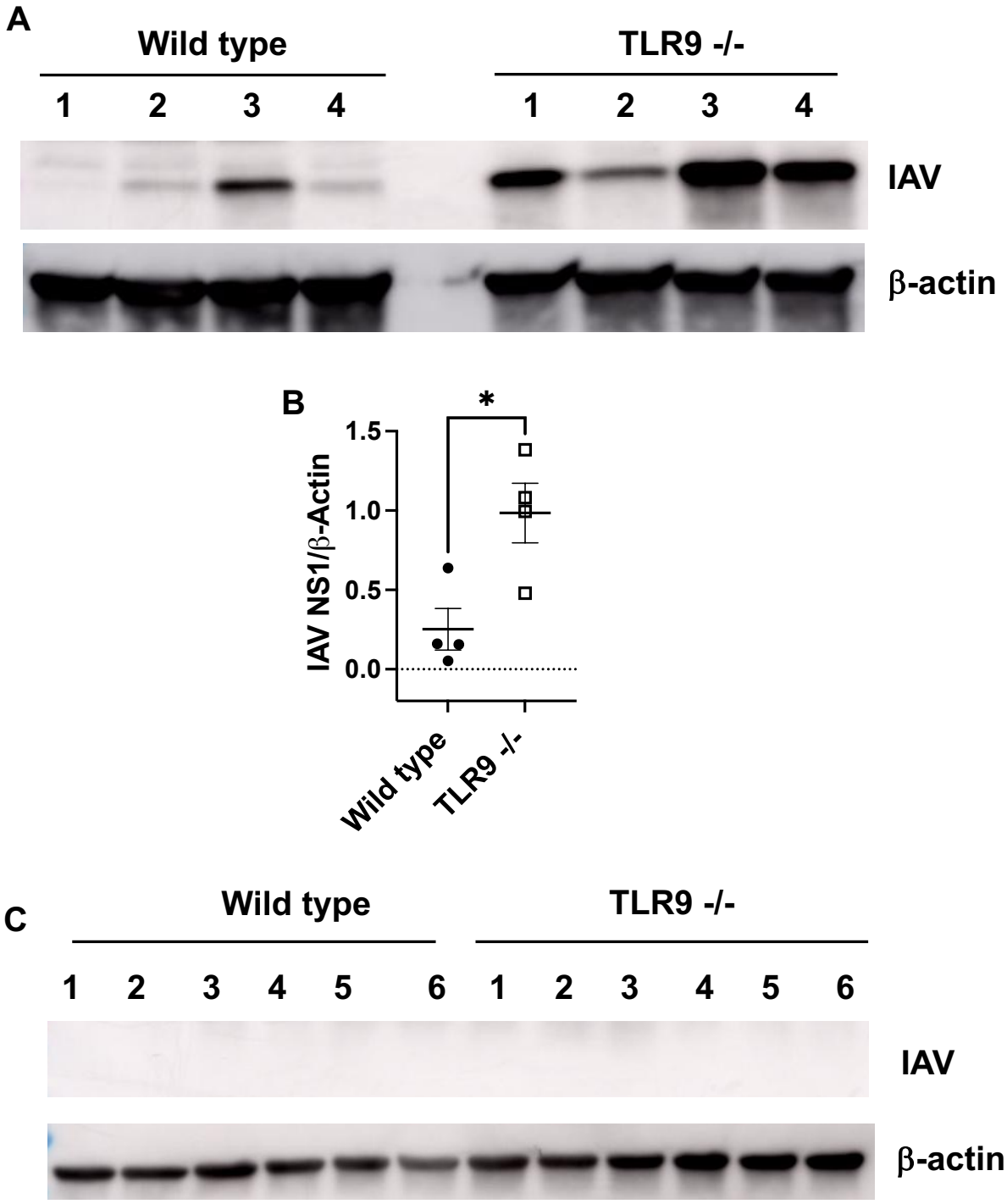

Supplemental Fig. 3. Western blot analysis of influenza NS1 protein on day 10 post-infection (A and B) and day 14 post infection (C).

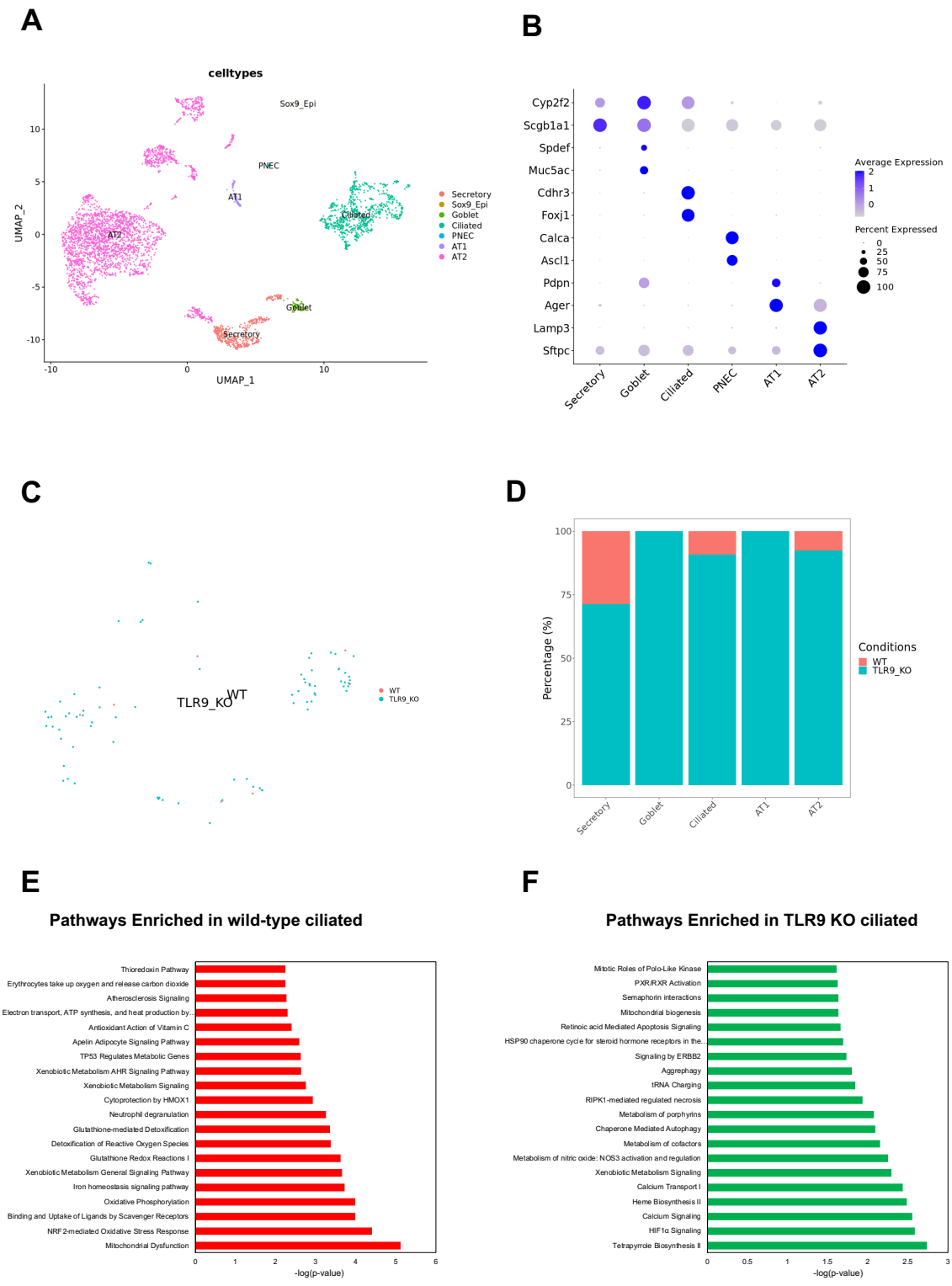

Supplemental Fig. 4. UMAP of epithelial cells in the lung (A) and markers to identify specific cell types (B). The identity of infected cells and associated genotype (C) and quantification (D). IPA pathway analysis showing enriched pathway in wild type and TLR9-/- ciliated epithelium

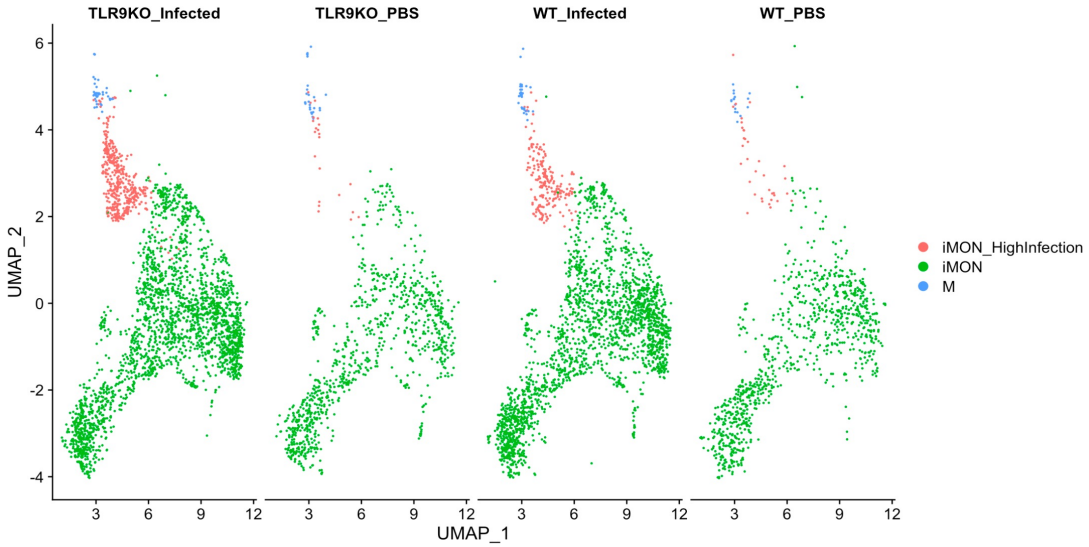

Supplemental Fig. 5. UMAP showing an expansion of iMON_Highinfection in infected mice, especially in TLR9-/- lungs.

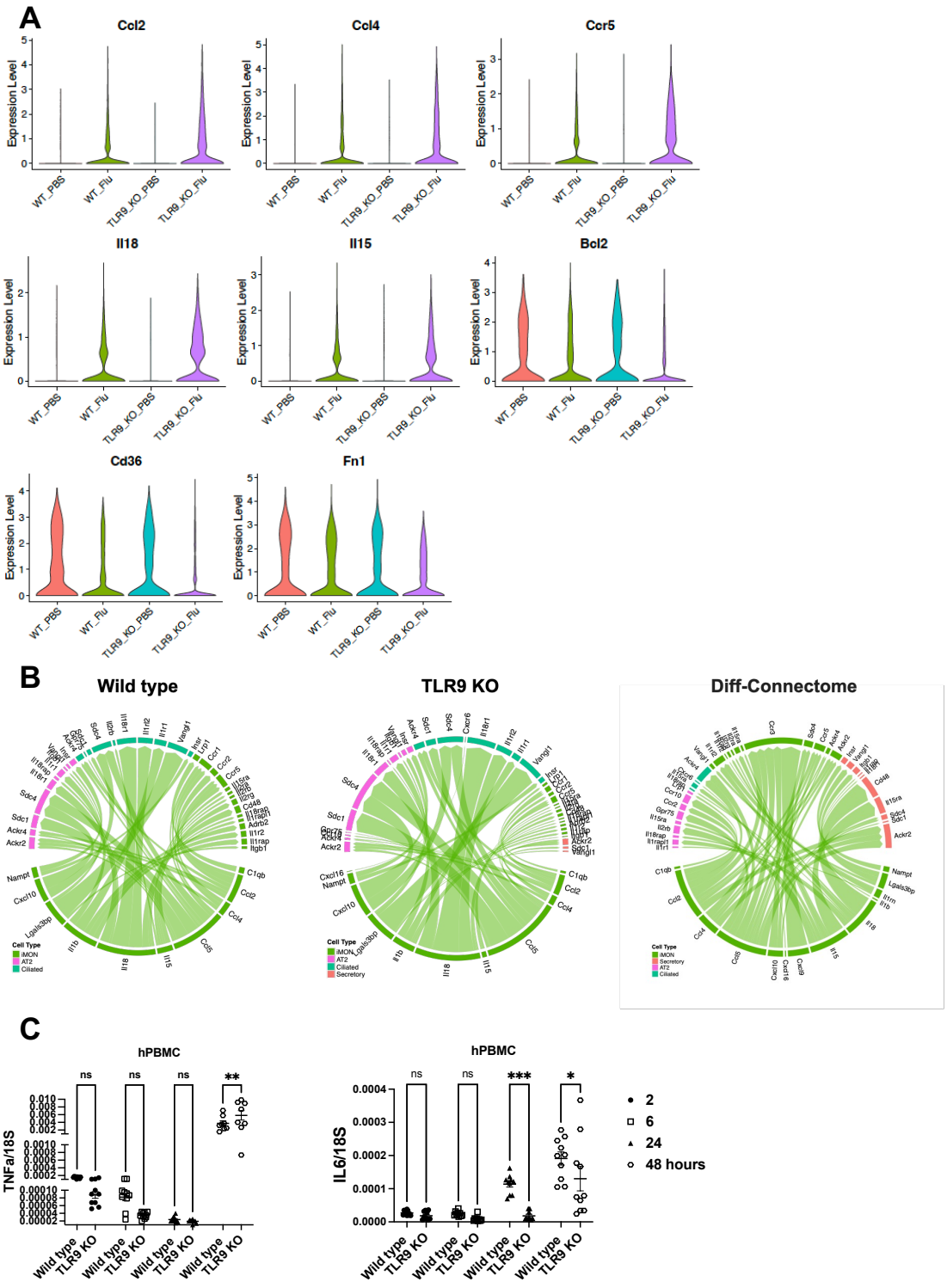

Supplemental Fig. 6. Violoin plots showing the expression levels of specific gene (A). Cell-cell communication analyses were performed using the R package Connectome. Average expression levels of ligands and receptors per cell type were computed across experimental groups. Connectomes were constructed for each experimental group, containing unfiltered lists of edges linking ligand-expressing cells to receptor-expressing cells. Diff-connectome was generated to demonstrated the upregulated receptor-ligand interactions in TLR9 KO cells (B). Human PBMC cell lines were infected with influenza (MOI of 1) and cytokine expressions were measured over the time course using qPCR (C). *, P < 0.05, **, P<0.01, and ***, P < 0.005 using two-way ANOVA.

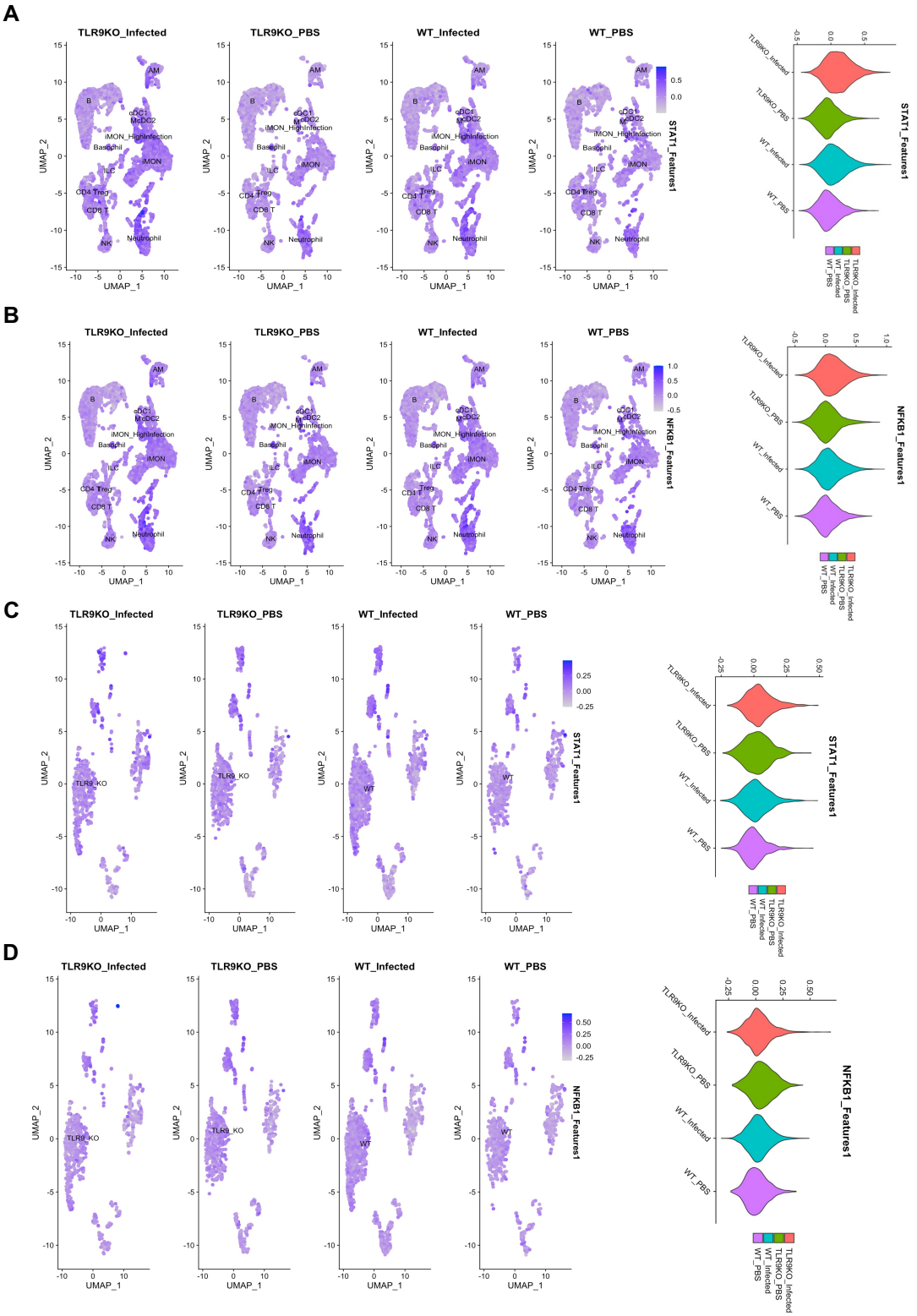

Supplemental Fig. 7. STAT1 and NFkB pathway signature in immune (A and B) and epithelial cells (C and D) along with respective quantifications on the right.

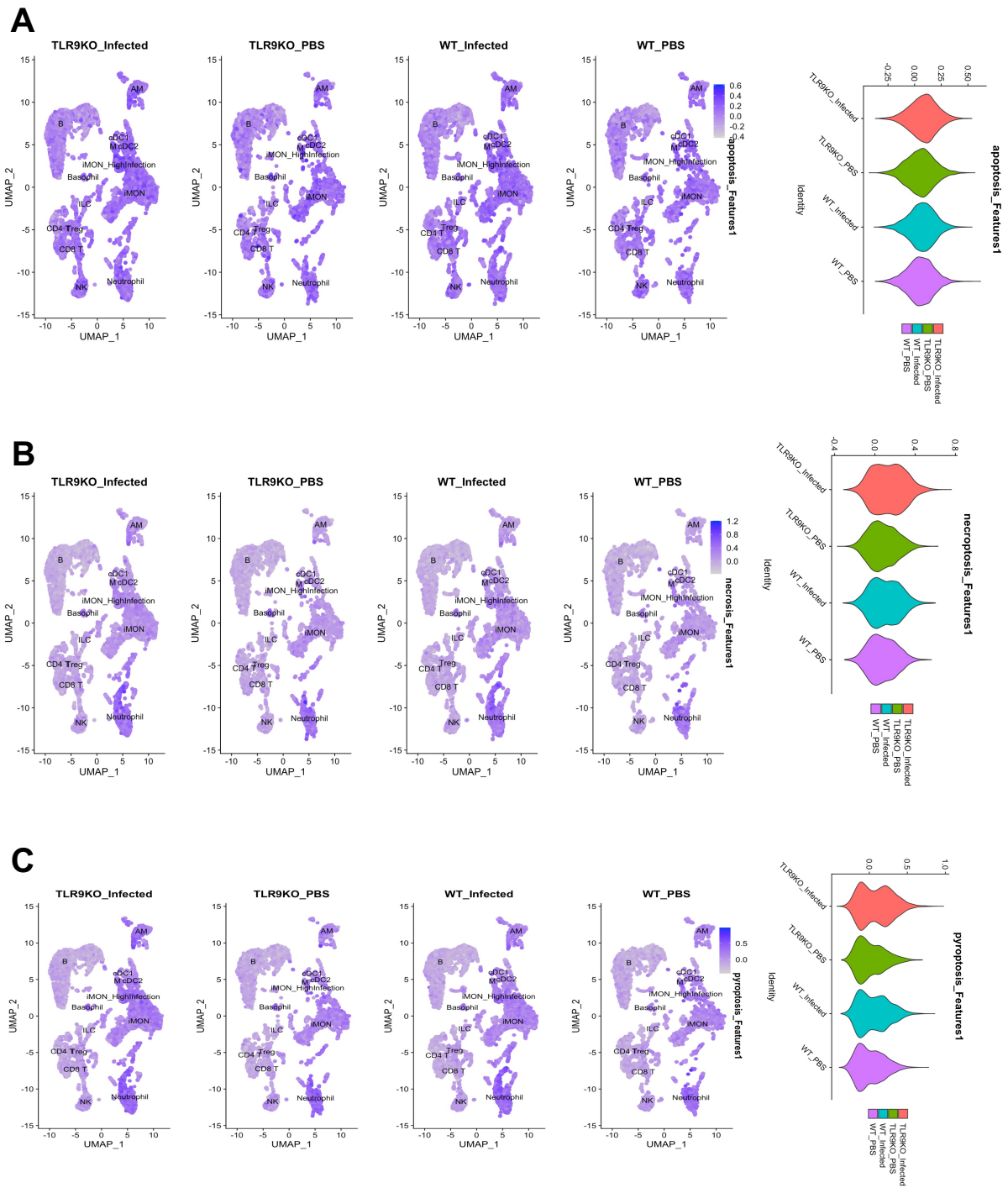

Supplemental Fig. 8. Apoptosis (A), necrosis (B), and pyroptosis (C) pathway signatures in immune cells along with respective quantifications on the right.

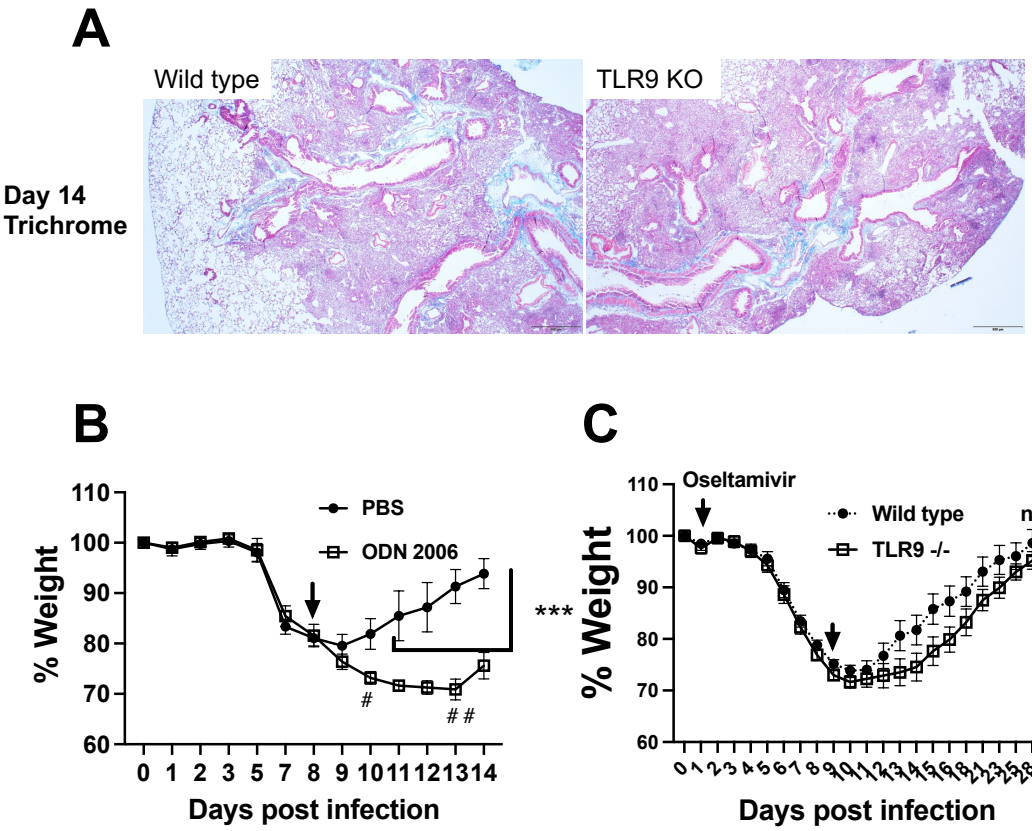

Supplemental Fig. 9. TLR9 stimulation post viral clearance impairs recovery: Histological analysis of lung tissue sections that were stained with trichrome staining to assess fibrosis (blue color) (A). Wild type mice were infected with influenza virus and randomized into two groups to either receive TLR9 agonist ODN2006 or PBS on day 8 by intranasal route. Body weights were measured every day. # indicates mortality in the ODN2006 on the indicated day (B). Wild type and TLR9-/- mice were infected with 4x dose (40 PFUs) of influenza virus and treated with oseltamivir every day (30 mg/kg) starting on day 1 post infection and until day 9 post infection. Body weights were measured (C). N=4-5 each group in A and 9-10 each group in B. ***, P<0.005 using two-way ANOVA with Šídák's multiple comparisons test, n= non-significant, # indicates one death on that day.

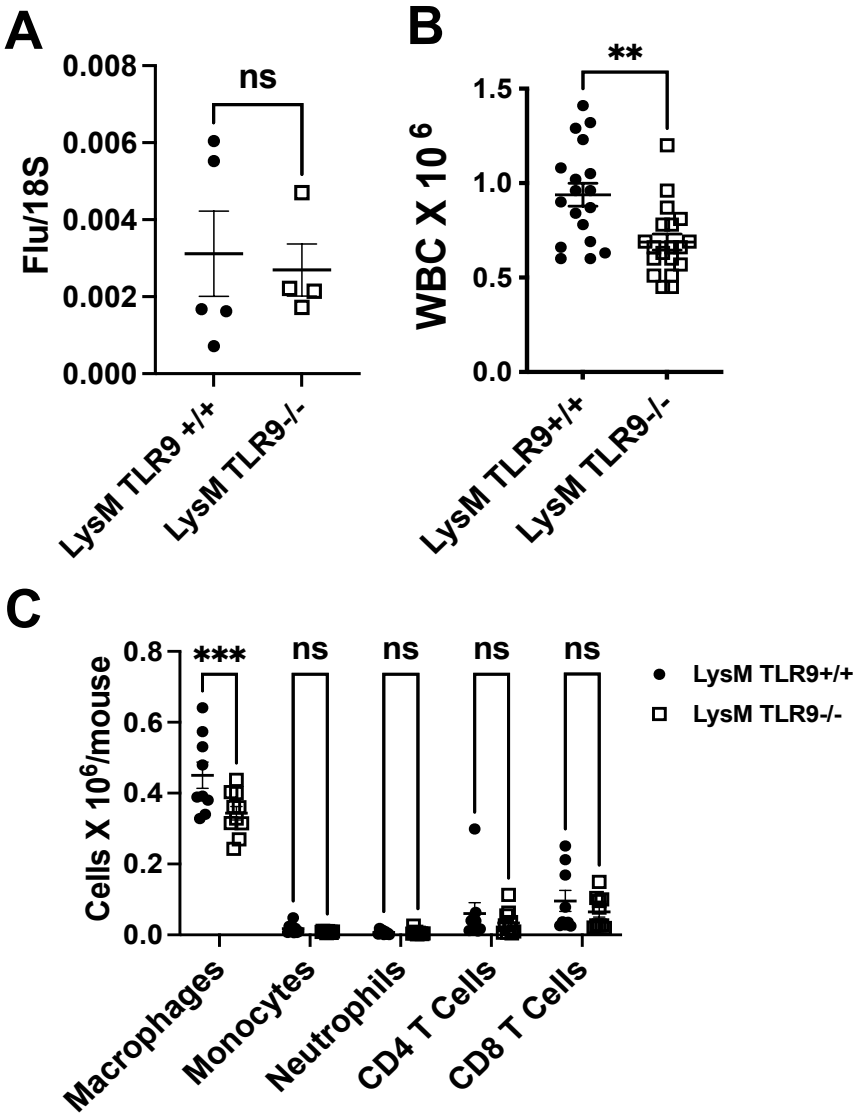

Supplemental Fig. 10. Myeloid specific TLR9 deficiency ameliorates lung inflammation without affecting viral clearance. LysM TLR9+/+ and LysM TLR9-/- were infected with influenza virus and euthanized on day 7 or day 14 to measure viral load and inflammation. Viral load was measured by qPCR on day 7 (A). Total WBCs were measured in the BAL samples harvested on day 14 (B) and specific cells were identified in a subset of experiments using flow cytometry (C). **, $P < 0.01$ using Mann-Whitney test and ***, $P < 0.005$ using two-way ANOVA.

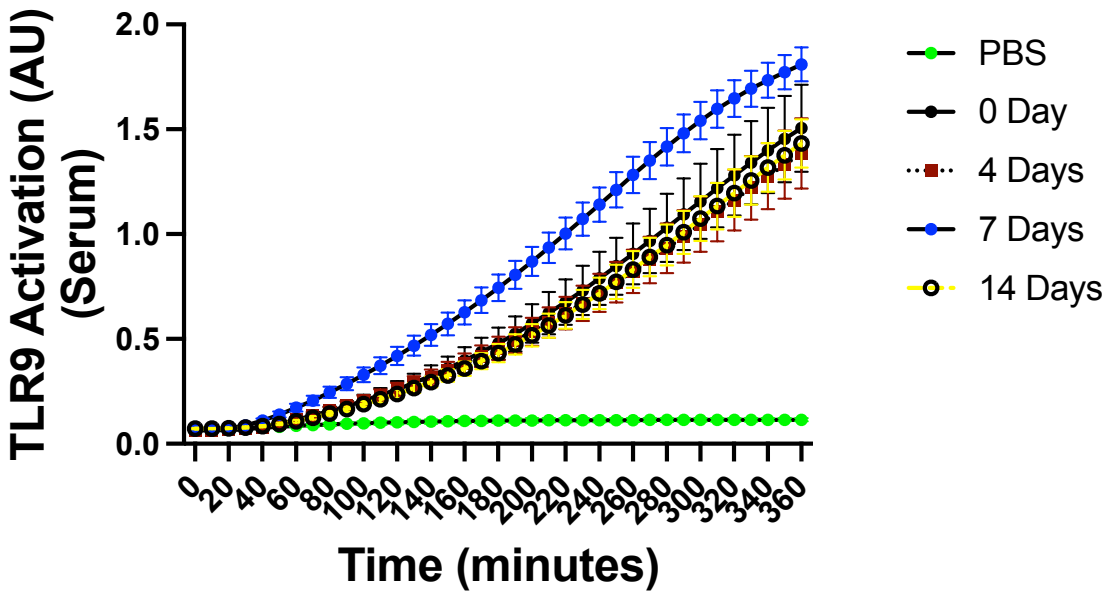

Supplemental Fig. 11. TLR9 activity was measured in mouse serum samples that were infected for 4, 7, or 14-days using mouse TLR9 reporter cell line. The data were measured using repeated measures for 6 hours. PBS alone served as a negative control. Day 7 values are statistically significant.